THE JOURNAL OF PHYSICAL CHEMISTRY C
A JOURNAL OF THE AMERICAN CHEMICAL SOCIETY

pubs.acs.org/JPCC

Article

Elucidation of a Metastable p(2 × 1) O Atom Adlayer Structure on Cu(111)

Audrey Dannar, Gunnar Louis Sly, Vinita Lal, Eva Peurrung, Volkan Cinar, Nisa Ulumuddin, Hojoon Lim, Adrian Hunt, Jean-Sabin McEwen,* Iradwikanari Waluyo,* and E. Charles H. Sykes*

Cite This: *J. Phys. Chem. C* 2024, 128, 19807−19814

Read Online

ACCESS | Metrics & More | Article Recommendations | Supporting Information

ABSTRACT: Cu-based catalysts are ubiquitous in many industrial reactions, including methanol synthesis. Under partially oxidizing conditions, Cu catalysts can have dynamic surface structures that greatly influence their reactivities. Therefore, elucidating the surface structures that are present on Cu, and looking for metastable structures, aids in the long term goal of understanding and controlling their catalytic behavior. Thin-film copper oxides such as the "29" and "44" structures have been described at length in the literature, but precursors to these thin-film oxides can be challenging to study because they exist only under certain conditions. Using a combination of experimental and computational surface science techniques, we discovered, modeled, and quantified a previously unreported O atom adlayer structure on Cu(111) with a p(2 × 1) unit cell. We used scanning tunneling microscopy to visualize the striped 2 × 1 structure and density functional theory (DFT) structure optimizations to identify the thermodynamically most favorable positions of Cu and O atoms in a p(2 × 1) unit cell. Using X-ray photoelectron spectroscopy and temperature-programmed desorption, we determined the stoichiometry of the structure to be 2:1 for surface Cu atoms to O adatoms, the same stoichiometry as that modeled by DFT. This work reports a new metastable structure formed on Cu(111) at the very initial stages of oxidation and is therefore worth considering in models of catalytically relevant redox processes at Cu surfaces.

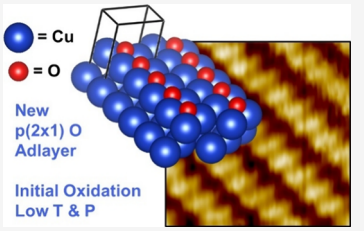

INTRODUCTION

Industrially important reactions such as the low-temperature water−gas shift reaction, methanol synthesis, and methanol steam reforming utilize Cu-based catalysts.[1−9] Some reactions can be promoted by the addition of O_2 to the reactant stream, for example, the water−gas shift reaction in methanol steam reforming.[4,9,10] However, it is not yet well understood what CuO_x species are formed from *in situ* O_2 exposure, which can make fundamental structure−function relationships in Cu-based catalysts difficult to determine. The oxidation of Cu(111) has been well-studied as an experimental model for the oxides formed during the *in situ* oxidation of Cu-based catalysts.[11−16] Above 170 K, O_2 dissociates on Cu(111) and, depending on the pressure and temperature, many different surface structures can form.[17,18] At initial or low exposures to O_2, dissociative adsorption leads to individual O atoms populating 3-fold hollow sites.[19] Oxidation of Cu(111) occurs most rapidly at surface step edges, and as O_2 exposure increases, undercoordinated Cu atoms at step edges diffuse to the lower terrace to form copper oxide patches below the steps.[20] Simultaneously to step edges, room-temperature oxidation of Cu(111) terraces is initiated at defect sites to produce a so-called *terrace oxide*, which appears in scanning tunneling microscopy (STM) images as triangular depressions.[21] Cu atoms are expelled from the terraces during the formation of terrace oxide, which are oxidized and present as *added oxide*, which appears in STM images as protruding islands.[21,22] These aforementioned oxygen structures formed at room temperature are typically found to be either polycrystalline or amorphous.

Above room temperature, a number of long-range, well-defined oxide thin films are known to form on Cu(111). Experimental model studies paired with density functional theory (DFT) computations have yielded detailed insight into two common Cu_2O-like structures known as the "29" and "44" oxides grown on Cu(111), with the "29" and "44" referring to the number of Cu atoms in the unreconstructed Cu(111) surface underlying each unit cell of the oxide.[23] The "44" and "29" oxides form at ∼423 and ∼673 K, respectively.[24,25] Interestingly, the "44" oxide can be annealed in vacuum to form the "29" oxide.[21] These oxides form unique structures that are commensurate with the Cu(111) lattice below, both of which are thought to consist of distorted hexagonal −O−Cu−O− rings on the Cu(111) surface with some O adatoms.[23] Recently, a combined theory and microscopy study proposed structures different from those accepted. Specially, their noncontact atomic force microscopy (AFM) study revealed

Received: July 3, 2024
Revised: October 23, 2024
Accepted: October 24, 2024
Published: November 11, 2024

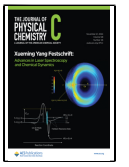

https://doi.org/10.1021/acs.jpcc.4c04452
J. Phys. Chem. C 2024, 128, 19807−19814

that ordered Cu vacancies in the "44" oxide and ordered Cu and O vacancies in the "29" oxide are present and appear in STM images as cavities in the lattices, rather than the pristine structures accepted previously.[26] The "29" oxide is the last thin-film oxide reported before the onset of bulk Cu_2O growth. Other metastable precursors such as the honeycomb,[23] "5−7",[27] and "8"[28] oxides exist, but these are stable over a smaller temperature and pressure range, are less well-ordered than the "29" and "44" oxides,[14,28−31] and less is known about their reactivities. Given that the structure and stoichiometry of copper oxide surfaces affect their chemical reactivity, knowledge about these precursor metastable oxides is important for more fully understanding catalytic mechanisms.

The fact that multiple copper oxide surface structures can form under the same conditions of exposure to O_2 complicates their study, and much remains to be understood about how they form and interconvert. Recently, a Cu_2O-like thin film was reported after exposing Cu(111) to O_2 at 400 K for 3 min, which is referred to as the "3 min" oxygen structure.[32] Schilling and co-workers hypothesized that the "3 min" structure was either incomplete or it consists of a mixture of oxide structures, making solving its structure challenging. In this publication, we describe a previously unreported ordered O atom adlayer structure on Cu(111) with a p(2 × 1) unit cell consisting of one O atom per two surface Cu atoms that must comprise part of the "3 min" surface grown at 400 K. The rows of this p(2 × 1) structure are commensurate with the Cu(111) high symmetry directions over ∼5 nm, and then a domain break occurs. Density functional theory indicates that the oxygen atoms bind to the 3-fold hollow sites as expected. Compared to the well-ordered "44" and "29" thin-film oxides, the p(2 × 1) structure is highly defective, existing in long and narrow ∼5 × 25 nm^2 domains with multiple domain boundaries, and is therefore of potential relevance to oxidative chemistry on Cu because defects are often the most reactive sites.[33,34]

MATERIALS AND METHODS

Scanning Tunneling Microscopy (STM). The samples were prepared for STM experiments in a preparation chamber ($P < 1 \times 10^{-9}$ mbar) connected to the STM chamber ($P < 1 \times 10^{-11}$ mbar) where images were obtained. A Cu(111) crystal (Princeton Scientific, 99.999% purity) was cleaned via alternating intervals of Ar^+ sputtering (1.5 keV beam energy, ∼10 μA drain current) and annealing to 900 K. The p(2 × 1) structure was formed by exposure to O_2 (5×10^{-6} mbar for 2−5 min = 451−1128 Langmuir (L)) either at 400 K or at room temperature, and the room-temperature samples were annealed to 400 K in the STM stage, at which point the p(2 × 1) structure formed. The annealing method was found to be a more reproducible way of forming the p(2 × 1) structure. STM images were obtained at room temperature with an etched W tip (Omicron Nanotechnology) with typical bias voltages of around −400 mV and tunneling currents of around 500 pA.

Temperature-Programmed Desorption (TPD). TPD experiments were performed in an ultrahigh vacuum (UHV) chamber with a base pressure of $<1 \times 10^{-10}$ mbar and equipped with a Hiden Hal/3F 301 RC quadrupole mass spectrometer for monitoring desorbing species as a function of surface temperature. All experiments were performed using a linear heating rate of 1 K/s. The Cu(111) crystal was mounted in the chamber via tantalum wires capable of being resistively heated to 750 K and cooled to 87 K via a liquid nitrogen cryostat. The crystal surface was cleaned by repeated cycles of Ar^+ bombardment using a hot filament sputter source and thermal annealing to 723 K. The "3 min" structure was prepared by exposing the clean Cu(111) surface to 5×10^{-6} mbar $^{16}O_2$ (99.999%, Praxair) at 400 K for 3 min. The "29" oxide surface, used as a quantitative control of stoichiometry, was prepared by exposing the Cu(111) surface to 5×10^{-6} mbar $^{16}O_2$ at 523 K for 3 min, which produces the same TPD results as the "29" oxide grown at 650 K and is within the DFT-derived phase diagram area for the "29" N = 5 structure.[25] Isotopic methanol CD_3OH (99.8%, Aldrich), which was freeze−pump−thawed prior to use, was used to quantify the oxygen coverage and was dosed at 87 K.

X-ray Photoelectron Spectroscopy (XPS). XPS experiments were conducted at the *In situ* and *Operando* Soft X-ray Spectroscopy (IOS) beamline located at port 23-ID-2 of the National Synchrotron Light Source II (NSLS-II) at Brookhaven National Laboratory. A description of the beamline and endstation is published elsewhere.[35] The Cu(111) crystal was cleaned using cycles of Ar^+ sputtering and annealing to 850 K until the surface was confirmed to be clean by XPS. The surface was exposed to 5×10^{-6} mbar of O_2 (Matheson, 99.994%) at 400 K for 3 min to prepare the "3 min" structure and at 650 K for 3 min to prepare the "29" oxide. XPS spectra were acquired at UHV and sample temperature of <350 K. O 1*s* and Cu 3*p* core levels were measured using a photon energy of 710 eV, and the binding energy was referenced to the Fermi edge.

Density Functional Theory (DFT). All DFT calculations were performed using the Vienna *Ab initio* Simulation Package (VASP) version 5.4.4.[36−38] Exchange correlation and electron-ion effects were treated using the generalized-gradient approximation (GGA) with the Perdew−Burke−Ernzerhof (PBE) functional.[39] PBE projector-augmented waves distributed in 2005[40−42] were employed, which considers the $2s^2 2p^4$ and the $4s^2 3d^9$ electrons explicitly in the valences for O and Cu, respectively. Electronic wave functions were expanded using a plane-wave basis set with kinetic energy cutoffs of 500 eV. A vacuum layer of 15 Å was used in these calculations. Further, a 8 × 16 × 1 Γ-centered Monkhorst−Pack k-point grid was used to sample the Brillouin zone of the Cu(111) p(2 × 1) unit cell, a 8 × 8 × 1 Γ-centered grid was used to sample the first Brillouin zone of the p(2 × 2) unit cell, and a 2 × 2 × 1 Γ-centered k-point grid was used for the isolated O/Cu(111) in a p(4 × 4) cell.[43] For the bulk calculations, 20 × 20 × 20 and 16 × 16 × 16 Γ centered k-point grids were used for the bulk Cu and bulk Cu_2O calculations, respectively. During convergence, the wave functions were considered self-consistent when the total energy differed by less than 10^{-4} eV and the geometries considered relaxed when the maximum force on any atom was less than 0.03 eV/Å. Entropic and zero-point vibrational entropy corrections were calculated by diagonalizing partial Hessian matrices constructed by using the finite-difference method with 0.015 Å displacements. For surface oxide structures, only atoms included in the oxide itself were considered in the partial Hessian. Methfessel−Paxton smearing with a width of 0.1 eV was used in all of the calculations. A converged Cu lattice constant of 3.636 Å was used to model all proposed surfaces and is consistent with the experimentally reported value of 3.62 Å.[44] The metastable Cu_2O p(2 × 1) surface was modeled by placing a single O adatom on a four-layered Cu(111) surface at the fcc site[45] to yield a 1/2 ML coverage. A variation on the previous 1/2 ML

https://doi.org/10.1021/acs.jpcc.4c04452
J. Phys. Chem. C 2024, 128, 19807−19814

O coverage surface was investigated by adding one Cu adatom to the p(2 × 1) unit cell, which was then optimized. An additional 1 ML CuO p(2 × 1) surface is proposed, which is modeled by placing two Cu and one O on the 1/2 ML surface. This surface represents two adatom O rows, with one row displacing a fifth Cu layer and yielding a square planar geometry with the displaced Cu layer akin to bulk CuO (Figure S4A). To verify that observations of the Cu_2O p(2 × 1) lattice shown later via STM are not larger than CuO_x p(2 × 2) surfaces with unobservable defects, the 1 ML CuO surface is extended to a 2 × 2 slab. Cu_4O_3 surfaces are modeled by removing a single surface oxygen atom (Figure S4C,G), and Cu_2O surfaces are modeled by removing two surface oxygen atoms (Figure S4E,F). In all geometry optimizations, the positions of the bottom two layers' positions are fixed. To examine the stability of these new proposed surfaces relative to other oxidized structures, the "29"oxide, bulk $Cu_2O(111)$, and honeycomb oxide models from Therrien et al. are compared.[25]

The stability of surface oxides can be studied via by calculating surface free energies of formation via

$$\gamma_f = \frac{1}{A}(G_{\text{oxide}} - G_{\text{bare}} - x\mu_{\text{Cu}} - y\mu_{\text{O}}) \tag{1}$$

where G_{oxide} and G_{bare} are the free energies of the oxide surface and bare surface, respectively.[46] x and y correspond to the number of Cu and O atoms per unit cell of area A with chemical potentials of μ_{Cu} and μ_{O}, respectively. Referencing the oxygen chemical potential $\mu_{\text{O}}(T, P_{\text{O}_2})$ to the DFT-calculated chemical potential at 298.15 K, 1 bar O_2 μ_{O} $(T^\circ, P^\circ_{\text{O}_2})$, we define a change in chemical potential $\Delta\mu_{\text{O}}(T, P_{\text{O}_2}) = \mu_{\text{O}}(T, P_{\text{O}_2}) - \mu_{\text{O}}$ $(T^\circ, P^\circ_{\text{O}_2})$. Here, we have that:

$$\mu_{\text{O}}(T^\circ, P^\circ_{\text{O}_2}) = \frac{E^{\text{DFT}}_{\text{O}_2}}{2} + \frac{E^{\text{ZPE}}_{\text{O}_2}}{2} + \frac{\mu^{\text{trans}}_{\text{O}_2}(T^\circ, P^\circ_{\text{O}_2})}{2} + \frac{\mu^{\text{vib}}_{\text{O}_2}(T^\circ)}{2} + \frac{\mu^{\text{rot}}_{\text{O}_2}(T^\circ)}{2} \tag{2}$$

where $E^{\text{ZPE}}_{\text{O}_2}$ is the zero-point energy of a spin-polarized O_2 molecule in the gas phase, $\mu^{\text{trans}}_{\text{O}_2}(T^\circ, P^\circ_{\text{O}_2})$ is the chemical potential for translations, and $\mu^{\text{rot}}_{\text{O}_2}(T^\circ)$ is the chemical potential for rotations for an O_2 molecule in the gas phase.[46] We note that once the reference chemical potential is set, $\mu_{\text{O}}(T, P_{\text{O}_2})$, for example, the pressure dependence is calculated by assuming an ideal gas:

$$\mu_{\text{O}}(T, P_{\text{O}_2}) = \mu_{\text{O}}(T, P^\circ_{\text{O}_2}) + \frac{1}{2}k_{\text{B}}T\ln\left(\frac{P_{\text{O}_2}}{P^\circ_{\text{O}_2}}\right) \tag{3}$$

Approximating the chemical potential of Cu μ_{Cu} as the total free energy of Cu per atom in the bulk, eq 1 can now be written as

$$\gamma_f = \frac{1}{A}(G_{\text{oxide}} - G_{\text{bare}} - x\mu_{\text{Cu}} - y\Delta\mu_{\text{O}}(T, P_{\text{O}_2}) - y\mu_{\text{O}}(T^\circ, P^\circ_{\text{O}_2})) \tag{4}$$

The conditions in which bulk oxidation of Cu is thermodynamically favorable can be studied by defining the free energy of oxidation as

$$\Delta G^{\text{bulk}}_{\text{ox}} = G^{\text{bulk}}_{\text{oxide}} - x\mu_{\text{Cu}} - y\mu_{\text{O}}(T, P_{\text{O}_2}) \tag{5}$$

With the stability criteria $\Delta G^{\text{bulk}}_{\text{ox}} < 0$, the range of bulk oxide chemical potentials can be written as

$$\frac{1}{y}(G^{\text{bulk}}_{\text{oxide}} - x\mu_{\text{Cu}} - y\mu_{\text{O}}(T^\circ, P^\circ_{\text{O}_2})) < \Delta\mu_{\text{O}}(T, P_{\text{O}_2}) \tag{6}$$

STM images of the modeled surfaces are generated at constant current using the Tersoff−Hamman approach as implemented within the program p4vasp.[47,48]

RESULTS AND DISCUSSION

Well-ordered crystalline surface oxide thin films like the so-called "44" and "29" oxides are typically grown at temperatures greater than 450 and 650 K, respectively, whereas oxidation of Cu(111) at or near room temperature typically results in the formation of disordered or very polycrystalline oxides.[21,24,25] We found that when Cu(111) was exposed to O_2 (5×10^{-6} mbar for 2−5 min, 450−1130 Langmuir (L)) at 400 K, or exposed to O_2 at room temperature and annealed to 400 K, a previously unreported ordered O atom adlayer structure formed (Figure 1). Figure 1A shows a large-scale scanning tunneling microscopy (STM) image of the Cu(111) surface after O_2 exposure at 400 K. On the left-hand side of Figure 1A, a boundary between the ordered structure (bright) and the disordered O/Cu terrace (dark) is seen. The majority of the surface consists of bright patches. Atomically resolved STM images reveal that the bright patches consist of multiple domains of the ordered row structures (Figure 1B) separated by domain boundaries, which appear darker in STM images. STM images from different parts of the surface reveal that these stripes run in one of the three high symmetry directions of the Cu(111) surface (Figure 1A). In Figure 1A, it can be seen that the individual domains of the ordered structure are relatively small and uniform in size; domain boundaries running normal to the rows are separated by an average distance of 5.4 ± 0.3 nm. The domain length running parallel to the rows is longer and more variable and is ∼25 nm on average. We hypothesize that the formation of the rows induces strain on the surface such that large domains cannot

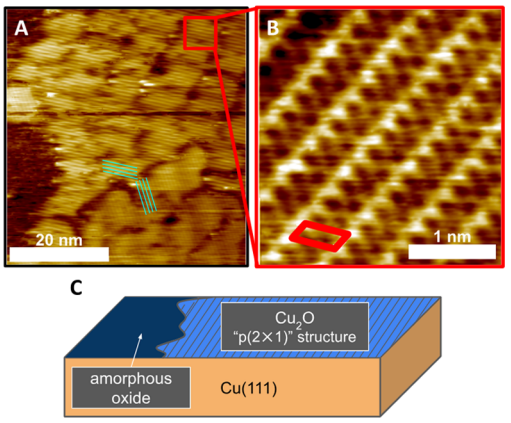

Figure 1. Characterization of the p(2 × 1) O adatom structure on Cu(111). (A) Large-scale room-temperature STM image of ∼15 domains of the p(2 × 1) O atom adlayer structure. The lighter areas are the p(2 × 1) structure, and darker areas (left) are disordered CuO_x. The cyan lines highlight adjacent rotational domains of the p(2 × 1) structure running 120° to each other. (B) Atomic-scale STM image of an individual p(2 × 1) domain with the unit cell marked in red. (C) Schematic representation of the STM image in panel (A).

https://doi.org/10.1021/acs.jpcc.4c04452
J. Phys. Chem. C 2024, 128, 19807−19814

form, and the critical domain size is related to the amount of strain built up before it becomes favorable to create a domain boundary. Adjacent domains need not have rows running in the same symmetry direction, as seen in Figure 1A, but we found that all domains consist of the same atomic-scale row structure with the same p(2 × 1) unit cell, which is shown in Figure 1B.

Atomic-scale STM images reveal that the stripes of the ordered structure are composed of two offset rows of depressions alternating with a single row of protrusions (Figure 1B). The experimentally measured unit cell depicted in Figure 1B was found to be 0.53 ± 0.03 × 0.25 ± 0.02 nm with 116 and 64 ± 5° angles, which fit within the expected values of 0.512 × 0.256 nm with 120 and 60° angles of a p(2 × 1) unit cell on Cu(111) (Table S1). Throughout this paper, we refer to this structure as the "p(2 × 1)" structure. Given the Cu(111) unit cell size is just two Cu atoms, the only possible oxygen coverages should be 1/2 or 1 ML as the only realistic O:Cu ratios are 1:2 or 1:1.

In an effort to determine the oxygen coverage of the "3 min" structure, we used X-ray photoelectron spectroscopy (XPS) to measure the O 1*s* peak area and compare it to the "29" oxide as a standard. Specifically, the Cu(111) crystal was exposed to 5 × 10^{-6} mbar O_2 at 400 or 650 K for 3 min to form either the "3 min" or "29" oxide. O 1*s* spectra for both surfaces, shown in Figure 2A, exhibit two distinct components, indicating that the O atoms are present in different environments. The spectra can be fitted with two peaks at 529.9 and 529.4 eV, which have been previously attributed to lattice O atoms and nonlattice, or likely adatom, O atoms, respectively.[49,50] The fact that the "3 min" structure contains both lattice and nonlattice O atoms is consistent with the fact that our STM results show that the p(2 × 1) generally coexists with several other structures. The smaller, broader tail on the high binding energy side arises from molecularly adsorbed H_2O (~533 eV) from the chamber background as well as a smaller amount of hydroxyl species (~531 eV).[48,49] The areas of the fitted peaks are shown in Table S3. To determine the total O coverage for the "3 min" sample, we found the ratio of the total O 1s peak areas for the "29" oxide to the "3 min" to be 1:0.875, inferring that the "3 min" oxide is essentially a Cu_2O surface but less oxygen dense than the "29" oxide, which was assumed to have a 2:1 Cu:O ratio. When assuming the DFT-derived benchmark "29" oxide Cu:O ratio of 29:17, the XPS determined Cu:O ratio for the "3 min" is found to be 2:1.02. These results similarly suggest a Cu_2O stoichiometry.

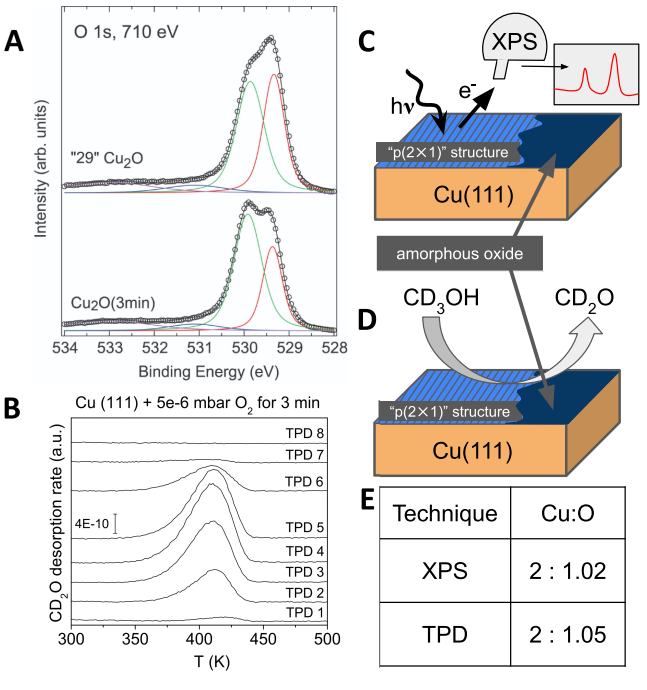

Figure 2. Quantitative XPS and TPD studies of oxygen surface coverage. (A) O 1*s* experimental spectra (circles) of the "29" (top) and "3 min" (bottom) surfaces and their peak fittings (solid lines). (B) TPD formaldehyde traces from methanol decomposition used as an independent way to quantify the oxygen coverage of the "3 min" and "29" surfaces. (C, D) Schematic representations of XPS and methanol titration experiments used to quantify the oxygen content of the surface. (E) Table depicting Cu:O ratios for the "3 min" sample obtained by XPS and TPD.

To validate the stoichiometry obtained by XPS, we utilized temperature-programmed desorption (TPD) to quantify the oxygen coverage of samples made using the same conditions, and again, the O coverage of the "29" oxide was used as a benchmark. The direct measurement of oxygen coverage on the Cu surface via recombinative desorption of O_2 is unreliable as oxygen can diffuse to the subsurface layer.[51−53] A precise method for quantifying the oxygen coverage of a thin-film oxide is titration of the oxide layer with a reductant and measuring the total amount of product, shown in the schematic in Figure 2D. We chose the partial oxidation of methanol (MeOH) to CH_2O as our titration reaction as the pristine Cu(111) surface is rather inert toward this reaction.[51,54] We performed the titration experiments using isotopically labeled MeOH (CD_3OH) and compared the results between the "3 min" and the "29" oxide, which has a proposed O atom density (0.586 ML).[25] Specifically, the Cu(111) surface was exposed to O_2 at the specific temperature and pressure needed to prepare each surface. The surface was then cooled to 87 K, exposed to ~4 L CD_3OH, and the temperature was ramped. O−H activation by surface oxygen results in a stabilized methoxy intermediate,[51] which either recombines with an H atom to form MeOH at higher temperature, or reacts further, desorbing as formaldehyde >400 K among other products.[51] Performing this titration multiple times until the surface was fully reduced while monitoring isotopically labeled formaldehyde production yielded a set of TPD traces such as those shown for the "3 min" sample in Figure 2B. The sequential reaction traces for the "3 min" and "29" samples were integrated, summed, and compared (Figure S1). For both surfaces, the formaldehyde desorption peak shifts to lower temperature in later TPD traces, which we attribute to the increasing number of defects (oxygen vacancies) as the surface is reduced, which is known to increase conversion to formaldehyde.[51] Upon analysis of the "29" and "3 min" surfaces via this method, an oxygen coverage of 0.526 ± 0.005 ML was found for the "3 min" surface in which the p(2 × 1) structure is observed. From this coverage, a stoichiometry of $Cu_2O_{1.05}$ was derived. This stoichiometry supports the XPS result that the "3 min" surface, and therefore presumably the p(2 × 1) structure, which is formed under these conditions, has a Cu_2O stoichiometry, as summarized in Figure 2E.

Based on the experimentally determined stoichiometry of Cu_2O for the p(2 × 1) structure and the observed ratio of 2 depressions to 1 protrusion in the STM images, we hypothesized that the protrusions are affiliated with the O

https://doi.org/10.1021/acs.jpcc.4c04452
J. Phys. Chem. C 2024, 128, 19807−19814

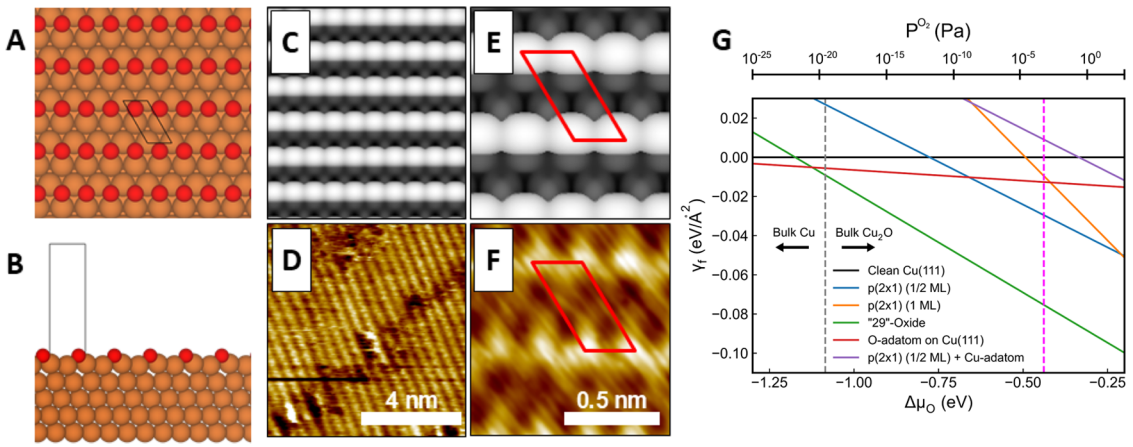

Figure 3. Density functional theory optimization of the p(2 × 1) structure and its thermodynamic stability. (A) Top-view of the p(2 × 1) O atom adlayer structure calculated by DFT. (B) Side view of the p(2 × 1) O atom adlayer on a Cu(111) slab. Orange spheres represent copper atoms, and red spheres represent oxygen atoms. (C−F) Simulated STM images (top) and experimental STM images (bottom) at a bias of −400 mV. Simulated STM images show Cu atoms as depressions and O atoms as protrusions. (G) Phase diagram as a function of $\Delta\mu_O$ for clean Cu(111) (black), "29" oxide (green), isolated O adatoms on Cu(111) (red), the proposed p(2 × 1) O atom adlayer (blue), an alternative p(2 × 1) 1 ML O atom adlayer (orange), an alternative p(2 × 1) structure with Cu adatoms (purple), and bulk Cu → Cu_2O transition (vertical, dashed gray). The vertical dashed magenta line shows the experimental conditions used for preparing the "3 min" sample: 400 K, 5 × 10^{-4} Pa (5 × 10^{-6} mbar).

adatoms. To further investigate the structure of the p(2 × 1) O atom adlayer, we performed DFT calculations on a p(2 × 1) model with surface oxygen atoms in 3-fold fcc hollow sites on Cu(111)[55] with the same spacing observed in STM images (Figure 3A−F). To identify the atomic-scale features in the p(2 × 1) structure observed by STM, we used DFT to simulate STM images of the optimized p(2 × 1) structure and compared these to experimental STM images recorded at a variety of tunneling gap voltages (Figure 3C−F and Figure S4). The simulated STM images show rows of bright protrusions centered over the O adatoms. Comparison of these DFT-simulated STM images (Figure 3C,E) with experimental STM images (Figure 3D,F) at both positive (not shown) and negative biases demonstrates good agreement with the experimental STM images and confirms the hypothesis that the protrusions observed in the STM images are the O atom sites.

To understand the thermodynamic stability of the p(2 × 1) structure compared with other possible structures, we used DFT calculations to generate a phase diagram and compare a set of candidate structures with different oxygen densities and structures over a range of O_2 pressures and temperatures of relevance to the experimental conditions reported herein (Figure 3G). Specifically, the "29" oxide[25] (green), bulk Cu_2O (vertical dashed gray), Cu(111) (black), an isolated O atom in 3-fold hollow site on Cu(111) (red), and the p(2 × 1) structure with different oxygen densities (1 ML O = orange, 1/2 ML O = blue) were compared. The corresponding structure of p(2 × 1) at 1 ML of O consists of both the adlayer O row and an additional subsurface O layer and is shown in Figure S4. Additionally, to examine if there is any reconstruction of the Cu(111) surface itself during the formation of the p(2 × 1) layer, we tested a 1/2 ML O p(2 × 1) structure with one Cu atom added to the unit cell (Figure 3G, purple line and Figure S5), but this structure was found to be even less thermodynamically stable than other test structures, which is attributed to unfavorable, acute O−Cu−O bond angles (Figure S5C). Interestingly, we find that the "29" surface oxide structure has a lower surface free energy as compared to the 1/2 ML O p(2 × 1) structure at the given experimental conditions (pink vertical line) (Figure 3G). The fact that the p(2 × 1) structure is less thermodynamically stable explains why we generally observe the p(2 × 1) among a mixture of other structures that changes as a function of temperature and O_2 pressure during sample preparation as seen in the STM image in Figure 1A and in Figure S3C−E. While additional surface oxide morphologies are observed and reported in the literature such as the "44," "5−7," and "8" oxides, they are not considered here as they have been calculated and compared on the Cu−O phase diagram prepared by Lee et al.[24] The authors employ a manual correction factor for the energy of isolated O_2 to account for its treatment via PBE, which shifts the chemical potentials to lower ranges relative to those prepared here; thus, a direct comparison of calculated conditions is unsuitable. However, in comparing relative energetics, it is clear that the oxide structures proposed, similar to the "29" oxide, are more stable than the prepared p(2 × 1) structure but adopt structures inconsistent with experimental STM, suggesting that formation of the reconstructed oxide structures is kinetically controlled.

The structure with the lowest surface free energy of formation at the relevant experimental conditions (Figure 3G, magenta dashed vertical line) matching the experimental STM images is the 1/2 ML coverage model depicted in Figure 3. To investigate the potential of surface stabilization from a combination of surface oxygen and unobservable subsurface oxygen atoms, a 1 ML variation of the p(2 × 1) model with a subsurface oxygen row was proposed (Figure 3G, orange line, and Figure S4A). DFT-generated STM images did not match the structure that was experimentally observed (Figure S6), nor agreed with the 1/2 ML O coverage derived from TPD and XPS.

To further investigate the possibility of stabilizing subsurface O atoms, we expanded the unit cell of the 1 ML structure to (2 × 2) to accommodate the removal of an O atom, optimized the structure, and generated the DFT-simulated STM image (Figure S4C,D).We optimized three additional defective 2 × 2 structures and generated a new phase diagram for comparison with the structures included in Figure 3G (Figure S4E−H). Two of the defective 2 × 2 structures had a single O atom

https://doi.org/10.1021/acs.jpcc.4c04452
J. Phys. Chem. C 2024, 128, 19807−19814

removed (Figure S4C,G), resulting in Cu_4O_3 stoichiometry. To match the experimentally measured Cu_2O stoichiometry, we removed two O atoms from each of the other defective 2 × 2 structures (Figure S4E,F). While three of the defective phases possessed lower surface free energies of formation (Figure S4H, orange, red, and purple lines), none of the proposed phases possessed morphologies consistent with experimental observations.

We conclude that the experimentally observed surface must be a metastable O adlayer, not a Cu surface reconstruction, which is consistent with early stages of oxidation.[12,14,56−58] For instance, deeper oxidation of Pd(111) proceeds via a chemisorbed surface O adlayer, which subsequently reconstructs and forms subsurface oxide with increasing O_2 exposure.[57] Such observations of kinetically controlled steps in the initial stages of metal surface oxidation are consistent with our findings that, under mildly oxidizing conditions, Cu(111) forms a p(2 × 1) metastable adlayer of O atoms that precedes known reconstructions like the "44" and "29" thin-film oxides and bulk Cu oxidation.

CONCLUSIONS

Under mildly oxidizing conditions, Cu surfaces form a variety of oxygen structures that coexist and dynamically interconvert. In this work, we have characterized a previously unreported p(2 × 1) structure observed at the initial stages of surface oxidation of Cu(111). We propose that this row-like structure seen in STM is a metastable, ordered O atom adlayer on Cu(111) with a p(2 × 1) unit cell. XPS and TPD were used to estimate the oxygen coverage of this structure, which by comparison to the "29" thin-film oxide was determined to be 1/2 ML. A variety of candidate structures were optimized with DFT, and their simulated images were compared with experimental STM images. The best match appears with a structure in which 1/2 ML O atoms occupy 3-fold hollow sites on Cu(111) in a p(2 × 1) overlayer. Phase diagrams generated from DFT calculations of a range of surface oxides indicate that the proposed p(2 × 1) structure is metastable with respect to other structures, but given our experimental observation that significant surface coverages of the p(2 × 1) structure can be generated near room temperature on Cu(111), it is important to consider. Given the impact of the structure of copper oxide surfaces on the reactivity, we suggest that this new structure may be of relevance to models that consider the population and reactivity of multiple oxide structures present under mildly oxidizing conditions.

ASSOCIATED CONTENT

Supporting Information

The Supporting Information is available free of charge at https://pubs.acs.org/doi/10.1021/acs.jpcc.4c04452.

STM measurements of the p(2 × 1) structure and unit cell, determination of O coverage by TPD and XPS, alternative p(2 × 1) adlayer structures, and phase diagram of the structures (PDF)

AUTHOR INFORMATION

Corresponding Authors

Jean-Sabin McEwen − *The Gene and Linda Voiland School of Chemical Engineering and Bioengineering, Department of Physics and Astronomy, Department of Chemistry, and Department of Biological Systems Engineering, Washington State University, Pullman, Washington 99164, United States; Institute for Integrated Catalysis, Pacific Northwest National Laboratory, Richland, Washington 99352, United States;* orcid.org/0000-0003-0931-4869; Email: js.mcewen@wsu.edu

Iradwikanari Waluyo − *National Synchrotron Light Source II, Brookhaven National Laboratory, Upton, New York 11973, United States;* orcid.org/0000-0002-4046-9722; Email: iwaluyo@bnl.gov

E. Charles H. Sykes − *Department of Chemistry, Tufts University, Medford, Massachusetts 02155, United States;* orcid.org/0000-0002-0224-2084; Email: charles.sykes@tufts.edu

Authors

Audrey Dannar − *Department of Chemistry, Tufts University, Medford, Massachusetts 02155, United States;* orcid.org/0009-0004-0534-6921

Gunnar Louis Sly − *The Gene and Linda Voiland School of Chemical Engineering and Bioengineering, Washington State University, Pullman, Washington 99164, United States*

Vinita Lal − *Department of Chemistry, Tufts University, Medford, Massachusetts 02155, United States*

Eva Peurrung − *The Gene and Linda Voiland School of Chemical Engineering and Bioengineering, Washington State University, Pullman, Washington 99164, United States*

Volkan Cinar − *Department of Chemistry, Tufts University, Medford, Massachusetts 02155, United States*

Nisa Ulumuddin − *The Gene and Linda Voiland School of Chemical Engineering and Bioengineering, Washington State University, Pullman, Washington 99164, United States*

Hojoon Lim − *National Synchrotron Light Source II, Brookhaven National Laboratory, Upton, New York 11973, United States;* orcid.org/0000-0001-5106-511X

Adrian Hunt − *National Synchrotron Light Source II, Brookhaven National Laboratory, Upton, New York 11973, United States;* orcid.org/0000-0002-5283-9647

Complete contact information is available at: https://pubs.acs.org/10.1021/acs.jpcc.4c04452

Notes

The authors declare no competing financial interest.

ACKNOWLEDGMENTS

Financial support for the experimental work at Tufts University was provided by the US Department of Energy, BES, Catalysis Science program under contract no. DE-SC0021196. This research used resources of the 23-ID-2 (IOS) beamline of the National Synchrotron Light Source II, a U.S. Department of Energy (DOE) Office of Science User Facility operated for the DOE Office of Science by Brookhaven National Laboratory under contract no. DE-SC0012704. Financial support for the theoretical work at Washington State University was provided by the National Science Foundation CAREER program under contract no. CBET-1653561. Computational resources were provided by the Kamiak HPC under the Center for Institutional Research Computing at Washington State University. We would like to thank Bjørk Hammer, David Duncan, and Philip Mousley for fruitful discussions. PNNL is a multiprogram national laboratory operated for the US DOE by Battelle.

REFERENCES

(1) Bickford, E. S.; Velu, S.; Song, C. Nano-structured CeO_2 supported Cu-Pd bimetallic catalysts for the oxygen-assisted water−gas-shift reaction. *Catal. Today* **2005**, *99* (3−4), 347−357.

(2) Fox, E. B.; Velu, S.; Engelhard, M. H.; Chin, Y.-H.; Miller, J. T.; Kropf, J.; Song, C. Characterization of CeO_2-supported Cu−Pd bimetallic catalyst for the oxygen-assisted water−gas shift reaction. *J. Catal.* **2008**, *260* (2), 358−370.

(3) Grabow, L.; Mavrikakis, M. Mechanism of methanol synthesis on Cu through CO_2 and CO hydrogenation. *ACS Catal.* **2011**, *1* (4), 365−384.

(4) Kugai, J.; Miller, J. T.; Guo, N.; Song, C. Oxygen-enhanced water gas shift on ceria-supported Pd−Cu and Pt−Cu bimetallic catalysts. *J. Catal.* **2011**, *277* (1), 46−53.

(5) Li, H.; Tian, H.; Chen, S.; Sun, Z.; Liu, T.; Liu, R.; Assabumrungrat, S.; Saupsor, J.; Mu, R.; Pei, C.; Gong, J. Sorption enhanced steam reforming of methanol for high-purity hydrogen production over Cu-MgO/Al_2O_3 bifunctional catalysts. *Appl. Catal., B* **2020**, *276*, No. 119052.

(6) Palo, D. R.; Dagle, R. A.; Holladay, J. D. Methanol steam reforming for hydrogen production. *Chem. Rev.* **2007**, *107* (10), 3992−4021.

(7) Ratnasamy, C.; Wagner, J. P. Water gas shift catalysis. *Catal. Rev.* **2009**, *51* (3), 325−440.

(8) Sekizawa, K.; Yano, S.-i.; Eguchi, K.; Arai, H. Selective removal of CO in methanol reformed gas over Cu-supported mixed metal oxides. *Appl. Catal., A* **1998**, *169* (2), 291−297.

(9) Utaka, T.; Sekizawa, K.; Eguchi, K. CO removal by oxygen-assisted water gas shift reaction over supported Cu catalysts. *Appl. Catal., A* **2000**, *194*, 21−26.

(10) González-Castaño, M.; Reina, T. R.; Ivanova, S.; Martínez Tejada, L. M.; Centeno, M. A.; Odriozola, J. A. O_2-assisted Water Gas Shift reaction over structured Au and Pt catalysts. *Appl. Catal., B* **2016**, *185*, 337−343.

(11) Eren, B.; Heine, C.; Bluhm, H.; Somorjai, G. A.; Salmeron, M. Catalyst chemical state during CO oxidation reaction on Cu(111) studied with ambient-pressure X-ray photoelectron spectroscopy and near edge X-ray adsorption fine structure spectroscopy. *J. Am. Chem. Soc.* **2015**, *137* (34), 11186−11190.

(12) Shi, S.; Han, Y.; Yang, T.; Zang, Y.; Zhang, H.; Li, Y.; Liu, Z. Ambient pressure X-ray photoelectron spectroscopy study of oxidation phase transitions on Cu(111) and Cu(110). *ChemPhysChem* **2023**, *24* (22), No. e202300543.

(13) Yang, J.; Kolasa, B.; Gibson, J.; Yeadon, M. Self-limiting oxidation of copper. *Appl. Phys. Lett.* **1998**, *73* (19), 2841−2843.

(14) Li, Y.; Chen, H.; Wang, W.; Huang, W.; Ning, Y.; Liu, Q.; Cui, Y.; Han, Y.; Liu, Z.; Yang, F.; Bao, X. Crystal-plane-dependent redox reaction on Cu surfaces. *Nano Res.* **2020**, *13*, 1677−1685.

(15) Gattinoni, C.; Michaelides, A. Atomistic details of oxide surfaces and surface oxidation: the example of copper and its oxides. *Surf. Sci. Rep.* **2015**, *70* (3), 424−447.

(16) Chen, H.; Curnan, M. T.; Liu, Q. F.; Ling, Y.; Lv, J.; Li, Y.; Huang, W.; Zhao, C.; Wang, R.; Gong, Z.; Cui, Y.; Han, J. W.; Yang, J. C.; Saidi, W. A.; Salmeron, M.; Yang, F. In situ visualization of cluster-mediated oxidation dynamics and kinetics on Cu(111), 2024

(17) Sueyoshi, T.; Sasaki, T.; Iwasawa, Y. Molecular and atomic adsorption states of oxygen on Cu(111) at 100−300 K. *Surf. Sci.* **1996**, *365* (2), 310−318.

(18) Wiame, F.; Maurice, V.; Marcus, P. Initial stages of oxidation of Cu (111). *Surf. Sci.* **2007**, *601* (5), 1193−1204.

(19) Besenbacher, F.; Nørskov, J. K. Oxygen chemisorption on metal surfaces: general trends for Cu, Ni and Ag. *Prog. Surf. Sci.* **1993**, *44* (1), 5−66.

(20) Zhou, G.; Luo, L.; Li, L.; Ciston, J.; Stach, E. A.; Yang, J. C. Step-edge-induced oxide growth during the oxidation of Cu surfaces. *Phys. Rev. lett.* **2012**, *109* (23), No. 235502.

(21) Matsumoto, T.; Bennett, R. A.; Stone, P.; Yamada, T.; Domen, K.; Bowker, M. Scanning tunneling microscopy studies of oxygen adsorption on Cu(111). *Surf. Sci.* **2001**, *471* (1−3), 225−245.

(22) Lawton, T. J.; Kyriakou, G.; Baber, A. E.; Sykes, E. C. H. An atomic scale view of methanol reactivity at the Cu(1 1 1)/CuO_x interface. *ChemCatChem* **2013**, *5* (9), 2684−2690.

(23) Jensen, F.; Besenbacher, F.; Lægsgaard, E.; Stensgaard, I. Oxidation of Cu(111): two new oxygen induced reconstructions. *Surf. Sci. Lett.* **1991**, *259* (3), L774−L780.

(24) Lee, Y.-J.; Ly, T. T.; Lee, T.; Palotás, K.; Jeong, S. Y.; Kim, J.; Soon, A. Completing the picture of initial oxidation on copper. *Appl. Surf. Sci.* **2021**, *562*, No. 150148.

(25) Therrien, A. J.; Zhang, R.; Lucci, F. R.; Marcinkowski, M. D.; Hensley, A.; McEwen, J.-S.; Sykes, E. C. H. Structurally accurate model for the "29"-structure of Cu_xO/Cu(111): A DFT and STM study. *J. Phys. Chem. C* **2016**, *120* (20), 10879−10886.

(26) Zhu, B.; Huang, W.; Lin, H.; Feng, H.; Palotás, K.; Lv, J.; Ren, Y.; Ouyang, R.; Yang, F. Vacancy ordering in ultrathin copper oxide films on Cu(111). *J. Am. Chem. Soc.* **2024**, *146* (23), 15887−15896.

(27) Yang, F.; Choi, Y.; Liu, P.; Stacchiola, D.; Hrbek, J.; Rodriguez, J. A. Identification of 5−7 defects in a copper oxide surface. *J. Am. Chem. Soc.* **2011**, *133* (30), 11474−11477.

(28) Richter, N. A.; Kim, C.-E.; Stampfl, C.; Soon, A. Re-visiting the O/Cu(111) system−when metastable surface oxides could become an issue! *Phys. Chem. Chem. Phys.* **2014**, *16* (48), 26735−26740.

(29) Therrien, A. J.; Hensley, A. J. R.; Zhang, R.; Pronschinske, A.; Marcinkowski, M. D.; McEwen, J.-S.; Sykes, E. C. H. Characterizing the geometric and electronic structure of defects in the "29" copper surface oxide. *J. Chem. Phys.* **2017**, *147* (22), No. 224706.

(30) Yang, F.; Choi, Y.; Liu, P.; Hrbek, J.; Rodriguez, J. A. Autocatalytic reduction of a Cu_2O/Cu(111) surface by CO: STM, XPS, and DFT studies. *J. Phys. Chem. C* **2010**, *114* (40), 17042−17050.

(31) Noh, J.-G.; Zong, K.-K.; Park, J.-B. Molecular-Scale investigation of reconstructed copper surface induced by dissociative adsorption of O_2. *Bull. Korean Chem. Soc.* **2011**, *32* (4), 1129−1130.

(32) Schilling, A. C.; Groden, K.; Simonovis, J. P.; Hunt, A.; Hannagan, R. T.; Çınar, V.; McEwen, J.-S.; Sykes, E. C. H.; Waluyo, I. Accelerated Cu_2O reduction by single Pt atoms at the metal-oxide interface. *ACS Catal.* **2020**, *10* (7), 4215−4226.

(33) Xu, F.; Mudiyanselage, K.; Baber, A. E.; Soldemo, M.; Weissenrieder, J.; White, M. G.; Stacchiola, D. J. Redox-mediated reconstruction of copper during carbon monoxide oxidation. *J. Phys. Chem. C* **2014**, *118* (29), 15902−15909.

(34) Soon, A.; Todorova, M.; Delley, B.; Stampfl, C. Thermodynamic stability and structure of copper oxide surfaces: A first-principles investigation. *Phys. Rev. B* **2007**, *75* (12), No. 125420.

(35) Waluyo, I.; Hunt, A. Ambient pressure X-ray photoelectron spectroscopy at the IOS (23-ID-2) beamline at the National Synchrotron Light Source II. *Synchrotron Radiat. News* **2022**, *35* (3), 31−38.

(36) Kresse, G.; Furthmüller, J. Efficient iterative schemes for ab initio total-energy calculations using a plane-wave basis set. *Phys. Rev. B* **1996**, *54* (16), 11169.

(37) Kresse, G.; Furthmüller, J. Efficiency of ab-initio total energy calculations for metals and semiconductors using a plane-wave basis set. *Comput. Mater. Sci.* **1996**, *6* (1), 15−50.

(38) Kresse, G.; Hafner, J. Ab initio molecular dynamics for liquid metals. *Phys. Rev. B* **1993**, *47* (1), 558.

(39) Perdew, J. P.; Burke, K.; Ernzerhof, M. Generalized gradient approximation made simple. *Phys. Rev. Lett.* **1996**, *77* (18), 3865.

(40) Lejaeghere, K.; Bihlmayer, G.; Bjorkman, T.; Blaha, P.; Blugel, S.; Blum, V.; Caliste, D.; Castelli, I. E.; Clark, S. J.; Dal Corso, A.; et al. Reproducibility in density functional theory calculations of solids. *Science* **2016**, *351* (6280), No. aad3000.

(41) Blöchl, P. E. Projector augmented-wave method. *Phys. Rev. B* **1994**, *50* (24), 17953.

(42) Kresse, G.; Joubert, D. From ultrasoft pseudopotentials to the projector augmented-wave method. *Phys. Rev. B* **1999**, *59* (3), 1758.

(43) Monkhorst, H. J.; Pack, J. D. Special points for Brillouin-zone integrations. *Phys. Rev. B* **1976**, *13*, 5188.

https://doi.org/10.1021/acs.jpcc.4c04452
J. Phys. Chem. C 2024, 128, 19807−19814

(44) Lide, D. R. *CRC handbook of chemistry and physics*; CRC press: 2004, Vol. *85*.
(45) Xu, Y.; Mavrikakis, M. Adsorption and dissociation of O_2 on Cu(111): thermochemistry, reaction barrier and the effect of strain. *Surf. Sci.* **2001**, *494* (2), 131−144.
(46) Collinge, G.; Kruse, N.; McEwen, J.-S. Role of carbon monoxide in catalyst reconstruction for CO hydrogenation: First-principles study of the composition, structure, and stability of Cu/Co($10\bar{1}2$) as a function of CO pressure. *J. Phys. Chem. C* **2017**, *121*, 2181−2191.
(47) Tersoff, J.; Hamann, D. R. Theory and application for the scanning tunneling microscope. *Phys. Rev. Lett.* **1983**, *50* (25), 1998.
(48) Tersoff, J.; Hamann, D. R. Theory of the scanning tunneling microscope. *Phys. Rev. B* **1985**, *31* (2), 805.
(49) Kahk, J. M.; Lischner, J. Core electron binding energies of adsorbates on Cu(111) from first-principles calculations. *Phys. Chem. Chem. Phys.* **2018**, *20* (48), 30403−30411.
(50) Mehar, V.; Huang, E.; Shi, R.; Rui, N.; Rosales, R.; Waluyo, I.; Hunt, A.; Liu, P.; Rodriguez, J. A. Microscopic investigation of H_2 reduced CuO_x/Cu(111) and ZnO/CuO_x/Cu(111) inverse catalysts: STM, AP-XPS, and DFT studies. *ACS Catal.* **2023**, *13* (14), 9857−9870.
(51) Russell, J., Jr; Gates, S. M.; Yates, J., Jr Reaction of methanol with Cu (111) and Cu(111)+ O (ads). *Surf. Sci.* **1985**, *163* (2−3), 516−540.
(52) Lee, S.; Mettlach, N.; Nguyen, N.; Sun, Y.; White, J. Copper oxide reduction through vacuum annealing. *Appl. Surf. Sci.* **2003**, *206* (1−4), 102−109.
(53) Bloch, J.; Bottomley, D.; Janz, S.; Van Driel, H.; Timsit, R. Kinetics of oxygen adsorption, absorption, and desorption on the Cu(111) surface. *J. Chem. Phys.* **1993**, *98* (11), 9167−9176.
(54) Pöllmann, S.; Bayer, A.; Ammon, C.; Steinrück, H.-P. Adsorption and reaction of methanol on clean and oxygen precovered Cu(111). *Z. Phys. Chem.* **2004**, *218* (8), 957−971.
(55) Pang, X.-Y.; Xue, L.-Q.; Wang, G.-C. Adsorption of atoms on Cu surfaces: a density functional theory study. *Langmuir* **2007**, *23* (9), 4910−4917.
(56) Ketteler, G.; Ogletree, D. F.; Bluhm, H.; Liu, H.; Hebenstreit, E. L.; Salmeron, M. In situ spectroscopic study of the oxidation and reduction of Pd(111). *J. Am. Chem. Soc.* **2005**, *127* (51), 18269−18273.
(57) Todorova, M.; Li, W.; Ganduglia-Pirovano, M. V.; Stampfl, C.; Reuter, K.; Scheffler, M. Role of subsurface oxygen in oxide formation at transition metal surfaces. *Phys. Rev. Lett.* **2002**, *89* (9), No. 096103.
(58) Li, L.; Liu, Q.; Li, J.; Saidi, W. A.; Zhou, G. Kinetic barriers of the phase transition in the oxygen chemisorbed Cu(110)-(2 × 1)-O as a function of oxygen coverage. *J. Phys. Chem. C* **2014**, *118* (36), 20858−20866.

https://doi.org/10.1021/acs.jpcc.4c04452
J. Phys. Chem. C 2024, 128, 19807−19814